



PERGAMON

Applied Mathematics Letters 14 (2001) 1005–1010

**Applied
Mathematics
Letters**

www.elsevier.nl/locate/aml

An Analysis of a Mathematical Model of Trophoblast Invasion

H. M. BYRNE

Department of Applied Mathematics
University of Nottingham
Nottingham NG7 2RD, United Kingdom

M. A. J. CHAPLAIN

Department of Mathematics
University of Dundee
Dundee DD1 4HN, United Kingdom

G. J. PETTET AND D. L. S. MCELWAIN

CiSSaIM, School of Mathematical Sciences
Queensland University of Technology
Brisbane, QLD 4001, Australia

(Received March 2000; accepted June 2000)

Communicated by W. Alt

Abstract—We present a mathematical model that describes the initial stages of placental development during which trophoblast cells begin to invade the uterine tissue. We then carry out a mathematical analysis of a simpler submodel that describes the final stages of normal embryo implantation and suggests that as the timescale of interest increases, the dominant migratory mechanism of the trophoblasts switches from chemotaxis to nonlinear random motion. © 2001 Elsevier Science Ltd. All rights reserved.

Keywords—Mathematical model, Placental development, Trophoblast invasion.

1. INTRODUCTION

The placenta plays an important role during mammalian pregnancy. By bringing the maternal and fetal blood networks into close proximity it ensures the efficient exchange of nutrients and waste products between mother and fetus. The formation of the placenta occurs in several stages [1–4]. Once the embryo has successfully attached to the uterine wall (\sim one week after fertilisation) trophoblast cells contained within the embryo invade the uterine stroma, secreting proteases that degrade the uterine tissue. The trophoblasts, perhaps in a response to the loss of contact inhibition, begin to proliferate and migrate into the uterine tissue as a continuous mass, with tips or protuberances forming at the invading front. Inhibitors expressed by the uterine tissue near the invading front [5] control the invasion process by binding with, and neutralising, the proteases. This stage of invasion usually continues until, on contact with the maternal decidua, the tips form anchoring villi. Trophoblast cells within the anchoring villi continue to proliferate

and form columnar aggregates. Individual trophoblast cells that break free from the anchoring villi migrate towards maternal blood vessels which they remodel, bringing about increased blood flow to the fetus.

In this paper, we study and analyse a mathematical model that describes the initial phase of placental development, when the trophoblasts invade as a continuous mass, and that was developed in [6]. Whereas in [6] attention focussed on constructing numerical solutions of the model, here the numerical results are used to develop a simplified or caricature model which enables us to focus on the way in which chemotaxis and nonlinear diffusion influence the migration of the trophoblasts at different stages during the invasion process. Indeed, a mathematical analysis of the reduced model leads us to predict that chemotaxis dominates trophoblast migration during early invasion and that it plays a role in defining the depth of penetration of the trophoblasts. However, nonlinear diffusion determines the ultimate steady state of the system.

2. THE MATHEMATICAL MODEL

Our one-dimensional model consists of four PDEs that govern the evolution of the invading trophoblasts $n(x, t)$, trophoblast-derived proteases $u(x, t)$, protease inhibitors $v(x, t)$, and uterine tissue $\rho(x, t)$ (for a detailed model derivation, see [6]). The equation for n contains terms describing random motion, chemotaxis, and proliferation (the trophoblasts are assumed to respond chemotactically to spatial gradients in v). The equations for u and v contain terms describing their diffusion, production, and neutralisation. The equation governing ρ contains terms describing its replacement and degradation by the protease. In appropriately scaled variables, the mathematical model is defined over the unit interval and written thus:

$$\frac{\partial n}{\partial t} = D_n \frac{\partial}{\partial x} \left(n^2 \frac{\partial n}{\partial x} \right) - \chi \frac{\partial}{\partial x} \left(n \frac{\partial v}{\partial x} \right) + k_1 n(1 - n - \rho), \quad (1)$$

$$\frac{\partial u}{\partial t} = D_u \frac{\partial^2 u}{\partial x^2} + k_2 u n(1 - n) - k_3 u v, \quad (2)$$

$$\frac{\partial v}{\partial t} = D_v \frac{\partial^2 v}{\partial x^2} + k_4 u \rho - k_3 u v, \quad (3)$$

$$\frac{\partial \rho}{\partial t} = k_5 \rho(1 - n - \rho) - k_6 u \rho, \quad (4)$$

where D_n is the cell random motility coefficient, D_u and D_v are chemical diffusion coefficients, χ a chemotaxis coefficient, and k_1, \dots, k_6 are kinetic rate parameters. To close the model, no-flux boundary conditions on n , u , and v are imposed at the uterine wall ($x = 0$) and at a characteristic distance inside the uterine tissue ($x = 1$, in dimensionless variables). We assume that initially the trophoblasts have penetrated a short distance into the uterine tissue and that the remaining space is occupied by uterine tissue ($\rho(x, 0) = 1 - n(x, 0)$). In addition, we assume that, initially, the protease and inhibitor are localised in pulses at, and a short distance ahead of, the leading trophoblast front.

The model equations were solved numerically using the method of lines and Gear's method as implemented by the NAG routine D03PGF. Two main types of behaviour were observed: either the trophoblasts penetrated a finite depth into the uterine tissue and then halted (see Figure 1) or they evolved to a steady travelling wavelike profile (see [6]). It was possible to switch from one type of behaviour to the other by changing a single parameter such as the rate of protease production (k_2) in equation (2).

3. A SIMPLIFIED MODEL

Guided by the results of Figure 1, we assume that during the later stages of normal implantation equations (2) and (4) reduce to give $u = 0$ and $\rho = 1 - n$. The model then simplifies to the

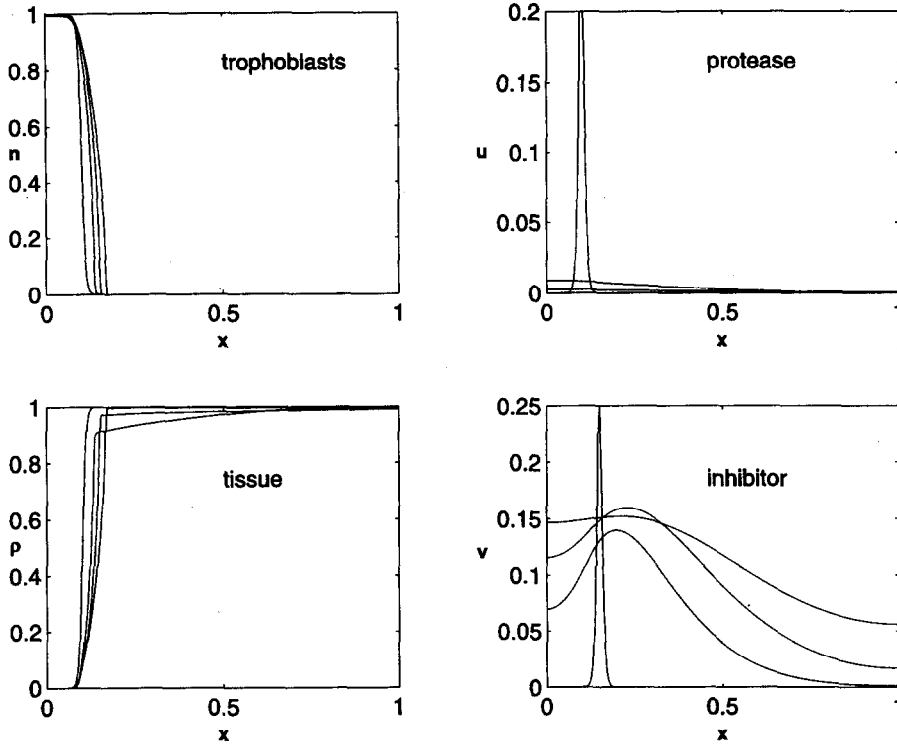


Figure 1. Here we present the results of a numerical simulation for which successful implantation occurs. The trophoblasts penetrate a certain depth into the uterine tissue and eventually halt. The dependent variables are plotted at times $t = 0, 1, 2, 3, 4$. Parameter values: $D_n = 0.001$, $D_u = 0.05$, $D_v = 0.01$, $\chi = 0.01$, $k_1 = 10$, $k_2 = 10$, $k_3 = 10$, $k_4 = 200$, $k_5 = 10$, $k_6 = 100$.

following two equations for n and v :

$$\frac{\partial n}{\partial t} = D_n \frac{\partial}{\partial x} \left(n^2 \frac{\partial n}{\partial x} \right) - \chi \frac{\partial}{\partial x} \left(n \frac{\partial v}{\partial x} \right), \tag{5}$$

$$\frac{\partial v}{\partial t} = D_v \frac{\partial^2 v}{\partial x^2}, \tag{6}$$

with $n_x = 0 = v_x$ at $x = 0, 1$ and initial profiles for v and n obtained from numerical simulations of the full model at some time $t = t_0$, say. The absence of any source or sink terms in (5),(6) leads us to suggest that during this stage of implantation, trophoblast proliferation and inhibitor production are negligible compared to trophoblast migration. In Figure 2, we present numerical simulations of (5),(6) which yield profiles for n and v that are in good agreement with simulations of the full model during the final stages of trophoblast implantation. In particular, as the inhibitor relaxes to a uniform steady state, the invasion of the trophoblasts is halted.

In order to proceed with the analysis of this simpler model, we note further that equation (6) is independent of n and can be solved analytically to determine $v(x, t)$. When this expression is substituted in (5) our model reduces to a single partial differential equation for n . On the basis of this simplified model, we predict that during the final stages of placental development the inhibitor initially controls the motion of the trophoblasts via chemotaxis. Once the inhibitor reaches a spatially uniform steady state, any subsequent motion of the trophoblasts is due to nonlinear random motion. In this respect, the specific form of $D_n(n)$ used in (5) is less important than the fact that $D_n(n) = D_n n^p$ where $p > 0$: we chose $p = 2$ as a simple representative example. The important feature is that compact support of the trophoblast profile is preserved—if we used $D_n(n) = D_n$, constant, then the trophoblasts would instantaneously penetrate the entire spatial domain which is not physically realistic. In the analysis which follows, we focus on two different

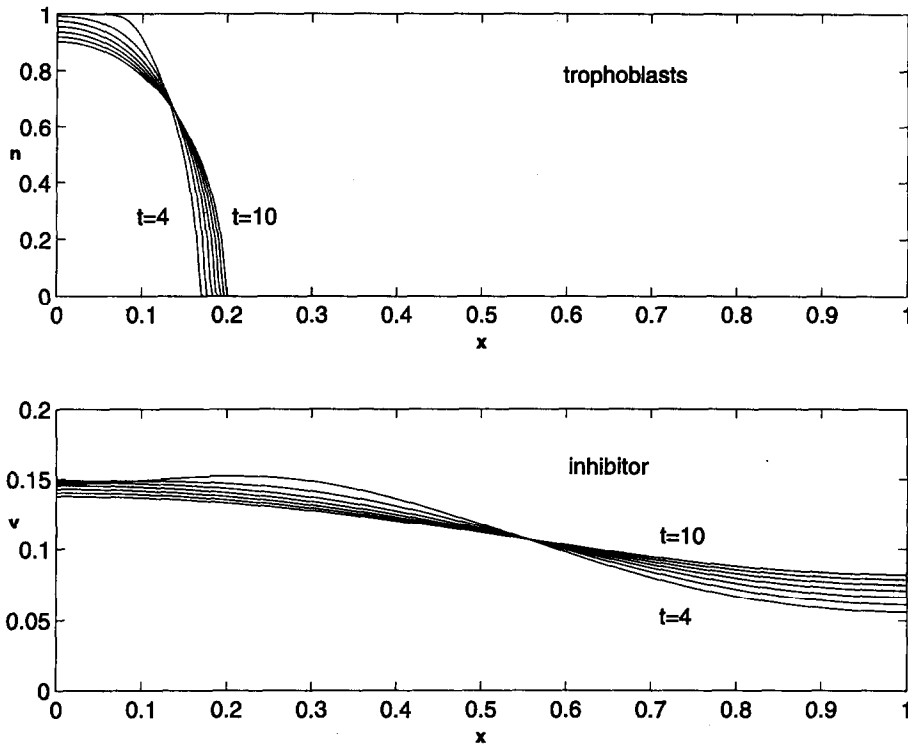


Figure 2. Here we present numerical results obtained using the reduced submodel. The profiles for the trophoblasts (n) and the inhibitor (v) are in good agreement with the corresponding simulations from the full model. The dependent variables are plotted at times $t = 4, 5, 6, 7, 8, 9, 10$. Parameter values: as per Figure 1, except that $u = 0$ and $\rho = 1 - n$.

timescales of interest for this simplified model: $t - t_0 \sim O(1)$ and $t - t_0 \rightarrow \infty$. We consider these cases separately below.

CASE 1. $t - t_0 \sim O(1)$. For small times, it is appropriate to solve (6) using the Green's function solution for the problem (see [7]), i.e.,

$$v(x, t) = \int_0^1 f(\xi)G(x, \xi, t - t_0) d\xi,$$

where $v(x, t_0) = f(x)$ and $G(x, \xi, t - t_0)$ is the Green's function for (6) satisfying the boundary conditions $v_x = 0$ at $x = 0, 1$ for $t > t_0$.

We note that the parameter values used in the numerical simulations satisfy $0 < D_n \ll \chi, D_v$. Therefore, taking $0 < D_n \ll 1$ as a small parameter, we now seek solutions to (5) of the form $n \sim n_0 + O(D_n)$, and at leading order we recover the following nonlinear hyperbolic equation:

$$\frac{\partial n_0}{\partial t} = -\chi \frac{\partial}{\partial x} \left(n_0 \frac{\partial v}{\partial x} \right). \tag{7}$$

Knowing the Green's function G above (which takes the form of an infinite series, cf. [7]), in theory we may now use a truncated form of the series (which should be valid for small time [7]) and solve the above nonlinear hyperbolic equation (7) using the method of characteristics [8]. The above analysis shows that initially chemotaxis is the dominant mechanism controlling cell migration.

CASE 2. $t - t_0 \rightarrow \infty$. For the long time solution to the problem (and guided by the results of Figure 2), we seek separable solutions (i.e., eigenfunction expansion) for $v(x, t)$ of the form

$$v(x, t) = \sum_{r=0}^{\infty} V_r \exp(-D_v r^2 \pi^2 (t - t_0)) \cos(r\pi x),$$

where the coefficients V_r are determined from the conditions specified at $t = t_0$, cf. [7], i.e.,

$$V_0 = \int_0^1 v(x, t_0) dx \quad \text{and} \quad V_r = 2 \int_0^1 v(x, t_0) \cos(r\pi x) dx, \quad r \geq 1.$$

We note that as $t - t_0 \rightarrow \infty$, the slowest decaying components of $v(x, t)$ will provide the dominant contribution to chemotaxis in (5). For this reason, and to minimise complexity, henceforth we shall assume that

$$v(x, t) \sim V_0 + V_1 e^{-D_v \pi^2 (t-t_0)} \cos(\pi x).$$

Substituting with this expression in (5) yields the following nonlinear partial differential equation that describes the long time evolution of the trophoblasts during the final stages of implantation:

$$\frac{\partial n}{\partial t} = D_n \frac{\partial}{\partial x} \left(n^2 \frac{\partial n}{\partial x} \right) + \chi \pi V_1 e^{-D_v \pi^2 (t-t_0)} \frac{\partial}{\partial x} (n \sin(\pi x)). \quad (8)$$

In the limit as $t - t_0 \rightarrow \infty$, the behaviour of the trophoblast cells is determined by setting $\frac{\partial}{\partial t} = 0$ in (8) and noting that $\frac{\partial v}{\partial x} \rightarrow 0$ as $t \rightarrow \infty$, i.e., $v \rightarrow \text{constant}$ solution and the chemotaxis effect is zero. (This can be deduced by applying the Maximum Principle for Parabolic PDEs, cf. [9].) In this case, it is possible to show, using similarity solution techniques, that $n(x, t) \sim \mathcal{N}(x)$, where

$$\mathcal{N}(x) \sim \begin{cases} \frac{4 \mathcal{N}^*}{3 L_\infty} \left(1 - \frac{x}{L_\infty} \right)^{1/3}, & 0 \leq x \leq L_\infty, \\ 0, & L_\infty < x. \end{cases}$$

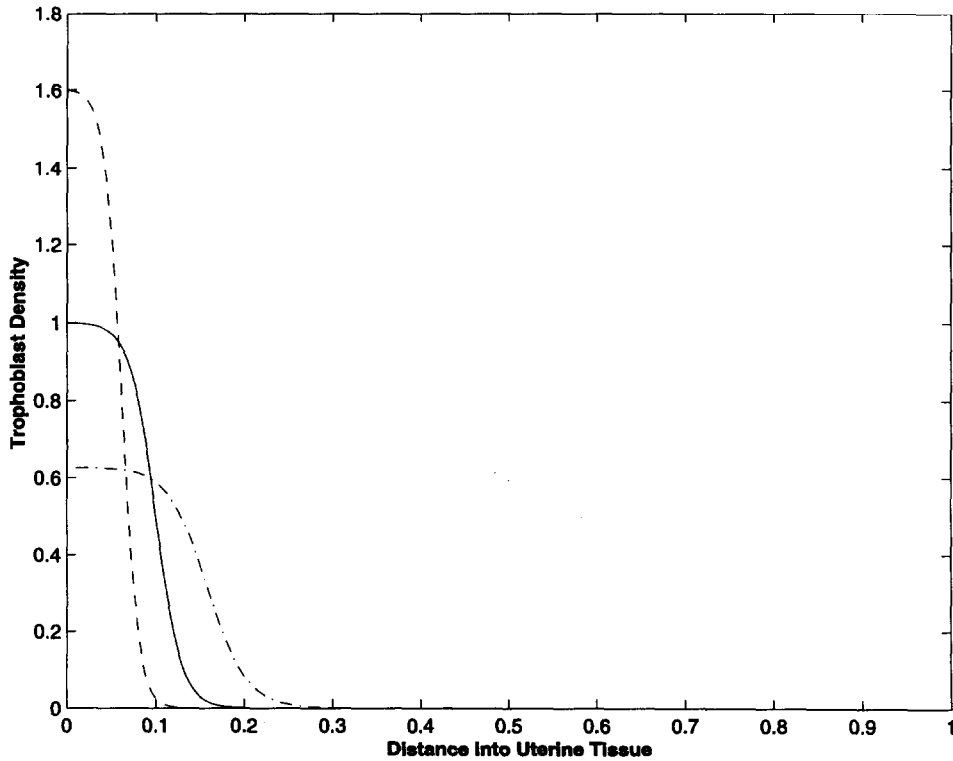


Figure 3. Here we present the results of a numerical simulation of equation (8) with initial trophoblast profile $n(x, 0)$ (solid line) and steady-state trophoblast profiles for $V_1 > 0$ ($= 5$) (dashed line, $- -$) as well as $V_1 < 0$ ($= -5$) (dot-dashed line $- \cdot - \cdot$). In particular, the asymptotic steady state trophoblast profiles reveal under-invasion when $V_1 > 0$ and normal propagation into the tissue when $V_1 < 0$ as predicted. The other parameter values used in each case were $D_n = 0.001$, $D_v = 0.01$, $\chi = 0.01$ (cf. Figure 1).

In this expression, \mathcal{N}^* represents the total number of trophoblast cells in the placenta and L_∞ is the depth of penetration. We determine \mathcal{N}^* by noting that for the reduced model the trophoblast population is fixed. Hence, we have

$$\mathcal{N}^* = \int_0^1 n(x, t) dx = \int_0^1 n(x, t_0) dx.$$

It is also clear from the above analysis of the submodel that, given an initial penetration depth L_0 , the limiting penetration depth L_∞ depends crucially on $\text{sign}(V_1)$. We anticipate that under normal circumstances the invading front of trophoblasts always propagates into the tissue (i.e., $V_1 < 0$). We also suggest that a possible mechanism for under-invasion ($L_\infty < L_0$), and subsequent rejection of the embryo (i.e., spontaneous abortion), is the establishment of an inhibitor concentration profile whose gradient causes a migration of trophoblasts out of the uterus (specifically $V_1 > 0$).

In order to substantiate this analysis, in Figure 3 we present some numerical simulations of equation (8) which verify the above findings. The figure shows two different steady state profiles of the trophoblast density—one steady state is achieved using a positive value of V_1 (in which case, we have under-invasion, as predicted), the other using a negative value of V_1 (in which case, we have propagation into the tissue, as predicted).

4. CONCLUSIONS

In this paper, we have presented a simple one-dimensional model that describes the early stages of placental development during which trophoblasts invade the uterine tissue as a continuous mass of cells. Analysis of a simplified model suggests that while chemotaxis drives the system towards its steady state, the precise details of the steady state are characterised by nonlinear diffusion. More precisely, chemotaxis is important in two ways. The initial invasion of the system is dominated by the chemotactic response of the trophoblast cells to the inhibitor v . In addition, when the protease is relaxing to a uniform steady state, chemotaxis plays an important role in defining the depth of penetration of the trophoblasts whilst the limiting profile adopted is determined by nonlinear random motility.

REFERENCES

1. T.D. Burrows, A. King and Y.W. Loke, Trophoblast migration during human placental implantation, *Human Reprod. Update* **2**, 307–321 (1996).
2. B.M. Carlson, *Human Embryology and Developmental Biology*, Mosby-Year Book, St. Louis, MO, (1994).
3. C.W.G. Redman, Cytotrophoblasts: Masters of disguise, *Nature Medicine* **3**, 610–611 (1997).
4. S. Strickland and W.G. Richards, Invasion of the trophoblasts, *Cell* **71**, 355–357 (1992).
5. M.B. Harvey *et al.*, Proteinase expression in early mouse embryos is regulated by leukaemia inhibitory factor and epidermal growth factor, *Development* **121**, 1005–1014 (1995).
6. H.M. Byrne, M.A.J. Chaplain, G.J. Pettet and D.L.S. McElwain, A mathematical model of trophoblast invasion, *J. Theor. Med.* **1**, 275–286 (1999).
7. J. Kevorkian, *Partial Differential Equations: Analytical Solution Techniques*, Chapman & Hall, London, (1990).
8. W. Williams, *Partial Differential Equations*, Oxford University Press, Oxford, (1980).
9. M.H. Protter and H.F. Weinberger, *Maximum Principles in Differential Equations*, Springer-Verlag, New York, (1984).
10. K.P. Conrad and D.F. Benyo, Placental cytokines and the pathogenesis of preeclampsia, *Am. J. Reprod. Immunol.* **37**, 240–249 (1997).
11. C.H. Graham and P.K. Lala, Mechanisms of placental invasion of the uterus and their control, *Biochem. Cell Biol.* **70**, 867–874 (1992).